Nano Biomed Eng
2020, 12(3): 191-196. doi: 10.5101/nbe.v12i3.p191-196.

Research Article

# Titania Nanotubes Arrays Based-Gas Sensor: $NO_2$-Oxidizing Gas and $H_2$-Reducing Gas

Ghufran Abd Al-Sajad[1], Araa Mebdir Holi[1], Asla Abdullah AL-Zahrani[2], Asmaa Soheil Najm[3]
[1]Department of Physics, College of Education, University of Al-Qadisiyah, Al-Diwaniyah, Al-Qadisiyah 58002, Iraq.
[2]Imam Abdulrahman-bin Fiasal University, Eastern Region, Dammam, Saudi Arabia.
[3]Department of Electrical Electronic and Systems Engineering, Faculty of Engineering and Built Environment, Universiti Kebangsaan Malaysia, 43600 UKM Bangi, Selangor, Malaysia.

Corresponding author. E-mail: araa.holi@qu.edu.iq

**Received:** Mar. 29, 2020; **Accepted:** Jun. 06, 2020; **Published:** Jul. 6, 2020

**Citation:** Ghufran Abd AL-Sajad, Araa Mebdir Holi, Asla Abdullah AL-Zahrani, and Asmaa Soheil Najm, Titania Nanotubes Arrays Based-Gas sensor: $NO_2$-Oxidizing Gas and $H_2$-Reducing Gas. *Nano Biomed. Eng.*, 2020, 12(3): 191-196.
**DOI:** 10.5101/nbe.v12i3.p191-196.

## Abstract

Gas sensor based on titanium dioxide ($TiO_2$) nanotube was manufactured and its sensitivity to hydrogen ($H_2$) and to nitrogen dioxide ($NO_2$) gasses was investigated using anodization method. The $TiO_2$ NT structure was studied using X-ray diffraction (XRD). The surface morphology of prepared Titania was analysed using field-emission electron-scanning microscopy (FE-SEM). Starting with (XRD) study it confirms the tetragonal phase structure of the prepared Titania (anatase and rutile). In addition, the $TiO_2$ anatase averaged crystallite size was 25.9 nm. The FE-SEM images revealed that the nanotube's average diameters are within 70 ± 2 nm. Gas response measurements at room temperature (27 °C) for hydrogen and nitrogen dioxide gases at various concentrations (100, 150, 200, 250 and 300 ppm) were investigated. Our study has shown that the higher resistance of $NO_2$ gas was 30 Ω at 300 ppm while it was equal 18.29 Ω at 150 ppm for $H_2$ gas at room temperature.

**Keywords:** Titania; Nanotube; Hydrogen; Nitrogen dioxide; Gas sensor

## Introduction

In recent years, due to low production costs, high sensitivity, ease of use and the ability to detect various gases, metal-oxide semiconductors (MOSs) have gained significant interest in the fields of environmental monitoring, automotive pollution control and food safety testing [1, 2]. There are two basic types of semi-conductive sensors based on metal oxides, n-type (whose majority carriers are electrons) and p-type (whose majority carriers are holes) [3]. The operating principle of MOS-based gas sensors is based on shifting the equilibrium of surface reactions associated with the analyte target. Usually, reducing gases like $NH_3$, CO, $H_2$, HCHO and others leads to increase in conductivity for n-type semiconductors and a decrease for p-type semiconductors, while the effects of oxidizing gases ($NO_2$, $O_3$, $Cl_2$, etc.) are reversed [4]. The $TiO_2$ nanostructures made from various nanoparticles, nanorods, nanowires, and nanotubes have received great attention in the gas exploration community due to their unique physical and chemical properties and their structural characteristic [5]. N-type semiconductors made from $TiO_2$ nanotubes [6] are considered one of the most promising materials because of their superior photocatalytic properties [7] and dilute photoelectrolysis [8] gas sensors [9] and dye-sensitized solar cells [10]. Titanium dioxide has

been synthesized using various chemical and physical processes. Various processing methods have been used to produce $TiO_2$ nanotubes, including hydrothermal synthesis [11], atomic layer deposition [12], pulsed laser deposition [13] and electrochemical anodization [14]. From this process, the electrochemical deposition of titanium is very interesting because it can produce an assembly structure at ambient temperature. In addition, $TiO_2$ nanotube arrays have very similar morphology, growth orientation, and large surfaces with controlled pore sizes [15]. In this study, $TiO_2$ nanotubes were obtained by anodizing in a solution containing ethylene glycol and ammonium fluoride and tested for their structure, optical properties and morphological composition. The morphological and structural investigations revealed that the as-grown $TiO_2$ nanotube were tetragonal and well crystallized. The resulting $TiO_2$ measuring device is exposed to $H_2$ and $NO_2$ gas at room temperature (27 °C). The experimental results have shown that the sensor shows an increase in $NO_2$ resistance and a decrease in $H_2$ resistance when the resistance is a function of working time at different concentrations.

# Experimental

## Fabrication $TiO_2$ nanotubes

First of all, Ti foil sheet (0.11 mm thick, 99.9% purity) was cut into 2.5×1 $cm^2$ pieces. Next, these pieces were chemically reduced by ultrasonic treatment in acetone, isopropanol or deionized water (DI) for 15 min, subsequently. Then, they were impressed in 6 M $HNO_3$ for 10 min to form a smooth surface. The anodizing technique of Ti foil was carried out in a high density two-electrode cell with high density graphite as the opposite electrode while the Ti foil acted as a working electrode. The distance between two electrodes was conserved at 2 cm. The two electrodes were connected to the power supply and immersed for 1 h at 40 V in an electrolyte consisting of 95 mL Ethylene glycol anhydrous + 5 mL DI + 0.5 g $NH_4F$ [16]. The prepared samples were rinsed with DI water. Thermo-oven was used to anneal the film up to 500 °C for 2 h [17].

The structure and phase of the sample were analysed by X-ray diffraction (Shimadzu 6000 diffractometer) using CuKα radiation (λ = 1.5406 Å) at 40 kV and 40 mA. Surface morphology and elemental analysis of $TiO_2$ nanotubes were tested using SUPRA 55 VP field emission scanning electron microscope (FESEM) to measure film thickness, surface morphology with acceleration voltages of 10 to 20 kV equipped with an energy dispersive X-ray detector (EDX).

## Gas sensing measurements

The geometry of the electrode from the titanium nanotube sensor is shown in Fig.1(a). The sensing was conducted using two platinum pads as electrodes at room temperature (27 °C). The sensing element was fabricated in a homemade chamber of flow type. The resistance was measured using an electrometer/high resistive meter of Keithley 6517A. The sensor temperature was monitored by a Lakeshore 340 temperature controller during measurements. The test chamber was first doused with high quality dry air at a steady flow rate of 100 to 300 ppm until the flow reached stable conditions. Nanotubes of $TiO_2$ were then exposed to both $H_2$ and $NO_2$. The desired concentration of $H_2$ was obtained via mass flow controller from the $H_2$ tube. $NO_2$ was obtained when the nitric acid ($HNO_3$) was heated at 50 °C.

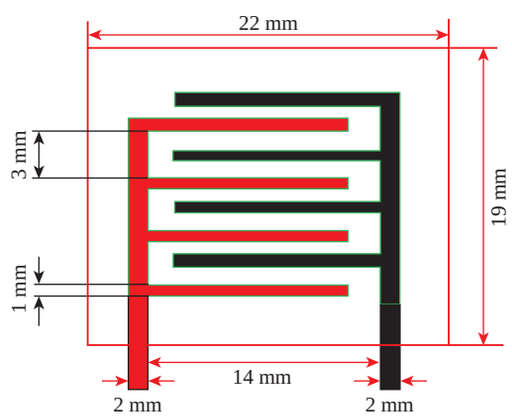


**Fig. 1** Schematic representation of the geometry of the electrodes.

# Results and Discussion

## Structural analysis

An X-ray diffraction pattern obtained from the calibration angle of a $TiO_2$ sample heated for 2 h at 500 °C in air is shown in Fig. 2. It is clear that anatase and rutile phases were present in the sample, where $TiO_2$ has been shown to have the wurtzite tetragonal structure. Peaks were combined with standard phase anatase and rutile $TiO_2$ and indexed tetragonal (JCPDS card number 00-021-1272) (JCPDS card number 00-021-1276). The anodized and annealed $TiO_2$ sample had sufficient crystallinity, and the highest peak was observed at 25.258° 2θ, an anatase level belonging to the lattice plane [101]. The crystallite size (D) at highest peak can be calculated by using Debye-

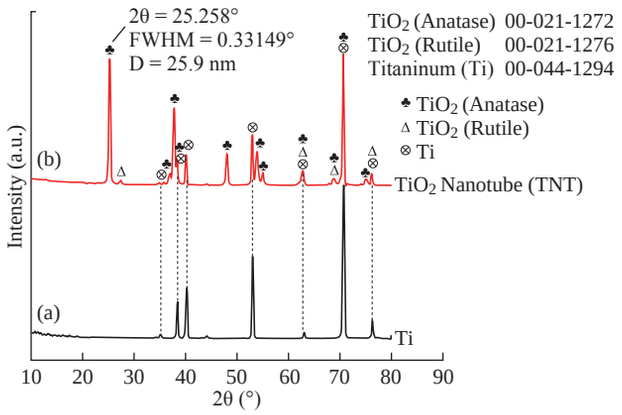


**Fig. 2** XRD patterns **(a)** Ti foil; and **(b)** $TiO_2$ nanotubes.

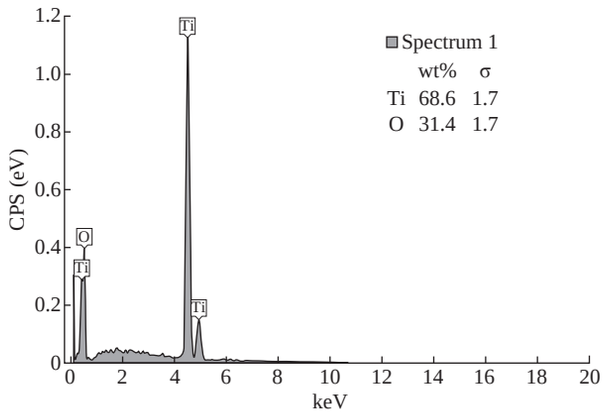


**Fig. 4** EDX spectrum of $TiO_2$ NTs.

Scherer's formula: $D = 0.9\lambda/\beta\cos\theta$ [18], and so the anatase average crystallite size for $TiO_2$ was found to be around 25.9 nm.

## Morphology analysis

The tube diameter of the samples was analyzed using image analysis software (Digimizer). The average dimeter of $TiO_2$ nanotube was 70 ± 2 nm. After 60 min of anodization time for Ti foil in prepared electrolyte, according to Fig. 3(a) which shows the FE-SEM image of this sample, the surface was quite filled with self-organized and well-ordered $TiO_2$ NTAs. Fig. 3(b) shows the cross-sectional image that the tubes were very smooth and aligned with length of around 2.100 ± 50 μm.

Fig. 4 shows the EDX spectrum that demonstrated

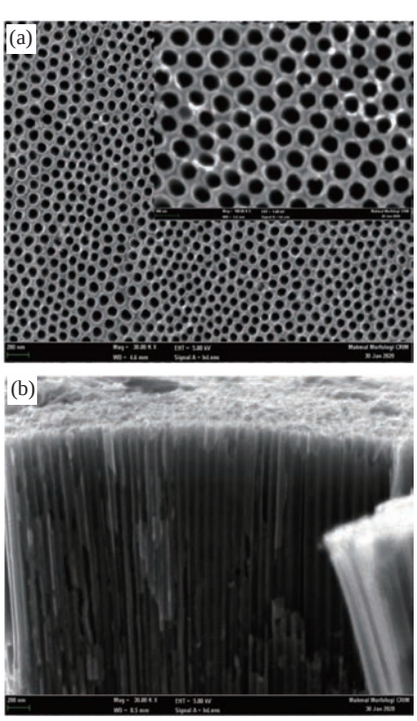


**Fig. 3** FE-SEM images of the $TiO_2$ NTs: **(a)** Top view and **(b)** cross-sectional.

the presence of titanium and oxygen elements. The ratio of Ti to O element was about 1:2 which thus established the construction of $TiO_2$ NTAs stoichiometry.

## Electrical properties

Hall effect measurements can be used to determine important material parameters, such as carrier mobility (μ), carrier concentration (n), Hall coefficient ($R_H$), resistivity (ρ), and the conductivity type (n or p), all derived from the Hall voltage measurement. The results obtained from the Hall Effect indicated that pure $TiO_2$ NTs had a negative Hall coefficient (–0.1272) with very low resistivity ($1.157\times10^{-4}$ Ω cm) and high mobility ($1.100\times10^{3}$ $cm^2/Vs$). Additionally, pure TNT conductive typically had carrier concentration of $-4.5\times10^{19}$ $cm^{-3}$ which was higher than the reported value of electron concentration of the pristine titania nanotubes as of $-1.55\times10^{16}$ $cm^{-3}$ [19].

## Sensing properties

The $TiO_2$ gas sensor is typical resistant-type that can increase resistance with oxidizing gas such as $NO_2$ gas [17]. The typical behavior of pure $TiO_2$ nanotubes arrays (TNTAs) when exposed to concentrations of $NO_2$ between 100 to 300 ppm is shown in Fig. 5. It is shown that the resistance increased with increasing concentration of $NO_2$. Higher resistance was observed for pure TNT at 300 ppm. Behavior of the sensor generated by TNT was constant and restored its original stability after repeated exposure to various concentrations of $NO_2$.

The adsorbed $NO_2$ is chemically absorbed in oxygen vacancies which form oxygen anions on the $TiO_2$ surface [20]. In the meantime, studies reported that $O^{2-}$ as the dominant chemisorbed species on $TiO_2$ [18], [20]. Consequently, oxygen adsorption was equivalent to

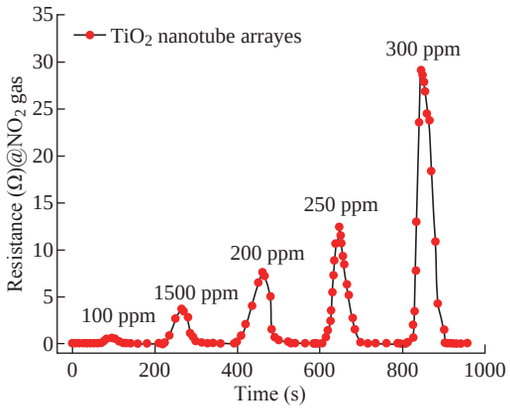


**Fig. 5** The resistance of pure TNTAs as a function of working time at different concentrations of nitrogen dioxide gas $NO_2$ at room temperature (27 °C).

oxygen ion sorption by taking nearby electrons on the $TiO_2$ surface, as defined in the following equation [21]:

$$NO_2(gas) + 2e^-(n\text{-type S.C.}) \rightarrow NO(gas) + O_2^-(ad.) \quad (1)$$

The diagram shown in Fig. 6 describes a condition in which $O_2$ was adsorbed on the $TiO_2$ polycrystalline surface.

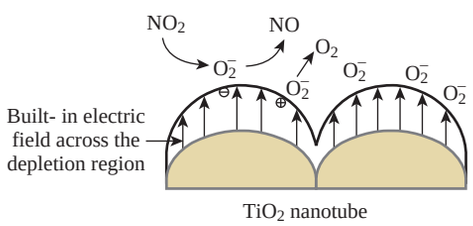


**Fig. 6** Schematic of the proposed $TiO_2$ sensor $NO_2$ gas sensing mechanism.

The $TiO_2$ gas sensor is a typical resistant-type sensor that can show a decrease in resistance to the reduced gas, such as $H_2$ gas [9]. Fig. 7 shows the response of the prepared pure TNT represented via changes in resistance as a function of working time. As revealed in this figure repeated exposure to hydrogen, the hydrogen concentration varies from 100 to 250 ppm at separate stages at ambient temperature in order to check the behaviour of the sensor. This behaviour confirmed that the sensor is constant and restores its original stability after repeated exposure to various concentrations of hydrogen gas. It was observed that due to the slow desorption rate, the magnitude of the response pulse decreased slightly with increasing concentration. The fundamental mechanism for sensor response is hydrogen ion chemisorption on the $TiO_2$ NTs thereby adsorption of protons on the surface, enhance the electron concentration, which is given in:

$$H_2 \rightarrow 2H^+ + 2e^- \quad (2)$$

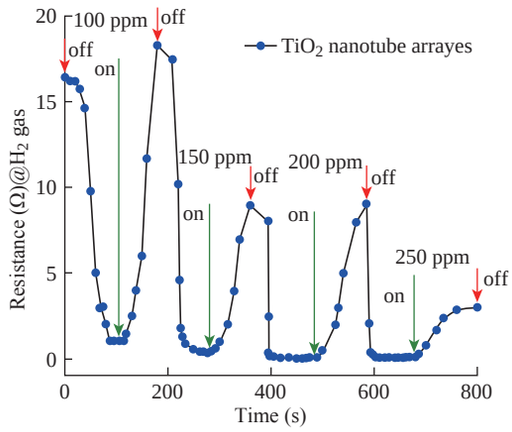


**Fig. 7** The resistance of pure TNTAs as a function of working time at different concentrations of hydrogen gas ($H_2$) at room temperature (27 °C).

The area of effective interaction between gas molecules and sensitive surfaces of $TiO_2$ determines the operation of the gas sensor. Increasing the ratio of surface area to volume of the inserted $TiO_2$ film improves the sensitivity of the sensor and dynamic characteristics [13]. Therefore, the dimensions of the $TiO_2$ nanotubes (diameter, length, and wall thickness) are proportional to the depth of the thinning layer significantly. The average diameter, length and wall thickness of the $TiO_2$ nanotubes were about 70 ± 2, 2100 ± 50 and 25 ± 5 nm, respectively. Thus, the adsorption of hydrogen in various concentrations (100 to 250 ppm) as a function of working time on the tube wall can cause the total depletion of electrons in the conductive band with a decrease in resistance. Another factor that may play a role in hydrogen sensitivity is the platinum electrode. Platinum can serve as a catalyst for the interaction of hydrogen with $TiO_2$ nanotubes. Hydrogen dissociation can occur at high temperatures on the platinum surface. These dissociated hydrogen atoms can diffuse to the surface of the nanotubes [14]. The $H_2$ macules react with chemisorbed oxygen at the TNT boundaries. A negative charge carrier (electron) is added to the TNT and hence the resistance decreases. Hence, the morphology of $TiO_2$ nanotubes plays efficient role to enhancing the gas sensing performance of both oxidized and reduced gases.

Fig. 8 shows response and recovery time as a function of changes in gas concentration of $NO_2$ and $H_2$ at ambient temperature. From Fig. 8(a), along with an increase in $NO_2$ gas concentration from 100 to 300 ppm, the response time values were fluctuating values; the increase in the concentration of $NO_2$ entailed a decrease in the response time. It was the shortest

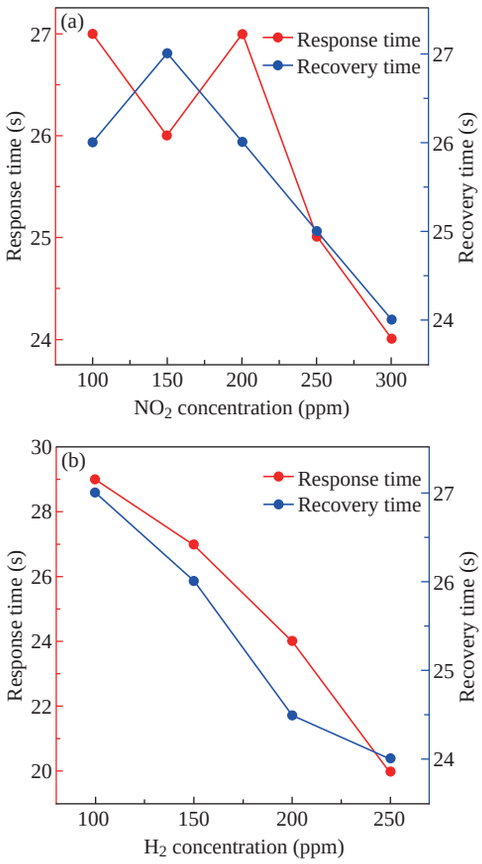


**Fig. 8** Response and recovery times of the $TiO_2$ nanotube sensor calculated for $NO_2$ and $H_2$ at different concentrations.

response time at 300 ppm. Once $NO_2$ gas was pumped and the TNT sensor surface hit, oxygen was adsorbed on the surface and the gas was diffused (sensor/chemical interface occurs). Desorption proceeded until all ions/particles of gas were removed from the interface. Until all gaseous ions/particles were separated from the system, desorption continued. The oxidizing gas ($NO_2$) interacted with chemically absorbed oxygen at the TNT material boundary. A negative charge carrier (electron) was taken from the TNT and hence the resistance increased. Also, Fig. 8(b) displays that the response and recovery time of TNT decreased as the concentration of the reducing gas $H_2$ increased. According to Gönüllü et al. [20], there were two ways to increase desorption, including boosting the temperature and injecting gas concentration at a higher level. Clearly the TNT sensor (Fig. 8(a) and (b)) provided short response and recovery time of 300 ppm and 250 ppm, respectively of $NO_2$ and $H_2$. Varghese et al. [22] reported that the $TiO_2$ nanotubes at 290 °C had a higher hydrogen sensitivity (1000 ppm $H_2$) with a response time of about 100 sec. Although Gönüllü et al. [21] stated that $TiO_2$ nano-tubular structure enhanced $TiO_2$ sensing capacity to a wider range of 400 °C $NO_2$ concentrations. Sensors consisting of titanium nanotubes prepared using anodization could thus be successfully used as hydrogen and nitrogen dioxide sensors based on our study and previous studies concluded.

## Conclusions

Titanium nanotubes were prepared by anodization and annealed in an oxygen atmosphere at a temperature of 500 °C. The average crystal size of $TiO_2$ was 25.9 nm at the vertices of the tetragonal shape. FE-SEM analysis was used to study surface morphology, and the resulting image showed the shape of radial tetragonal nanotubes. The nanotube sensors contained anatase and rutile titanium phases and were significantly resistant depending on the operating time at different concentrations of hydrogen gas $NO_2$ and $H_2$ at room temperature (27 °C), which was 30 Ω and 18.29 Ω, respectively. This sensory behavior in $TiO_2$, which was not limited to $NO_2$ sensors, could mainly be associated with the structure of the sensor material and good contact with the substrate and the location of the electrodes. It is believed that the water-resistance of nanotubes is based on hydrogen chemisorption which acts as an electron donor on the surface of the titanium. In summary, it has been shown that sensors made from titanium nanotubes made by anodizing can be successfully used as $H_2$ and $NO_2$ sensors.

## Conflict of Interests

The authors declare that no competing interest exists.

## References

[1] X. He, J. Li, X. Gao, et al., $NO_2$ sensing characteristics of $WO_3$ thin film microgas sensor. *Sensors Actuators, B Chem.*, 2003, 93: 463-467.

[2] S. Bai, D. Li, D. Han, et al., Preparation, characterization of $WO_3$-$SnO_2$ nanocomposites and their sensing properties for $NO_2$. *Sensors Actuators, B Chem.*, 2010, 150: 749-755.

[3] G.F. Fine, L.M. Cavanagh, A. Afonja, et al., Metal oxide semi-conductor gas sensors in environmental monitoring. *Sensors*, 2010: 5469-5502.

[4] J. Zhang, Z. Qin, D. Zeng, et al., Metal-oxide-semiconductor based gas sensors: Screening, preparation, and integration. *Phys. Chem. Chem. Phys.*, 2017, 19: 6313-6329.

[5] V. Galstyan, E. Comini, G. Faglia, et al., $TiO_2$ nanotubes: Recent advances in synthesis and gas sensing properties. *Sensors (Switzerland)*, 2013, 13: 14813-14838.

[6] G. Eranna, B. C. Joshi, D.P. Runthala, et al., Oxide materials for development of integrated gas sensors - a comprehensive review. *Critical Reviews in Solid State and Materials Sciences*, 2004, 29: 111-188.
[7] K. Eufinger, D. Poelman, H. Poelman, et al., $TiO_2$ thin films for photocatalytic applications. *Thin Solid Films: Process and Applications*, 2008, 37661: 2.
[8] G.K. Mor, O.K. Varghese, M. Paulose, et al., A review on highly ordered, vertically oriented $TiO_2$ nanotube arrays: Fabrication, material properties, and solar energy applications. *Sol. Energy Mater. Sol. Cells*, 2006, 90: 2011-2075.
[9] D. Aphairaj, T. Wirunmongkol, S. Niyomwas, et al., Synthesis of anatase $TiO_2$ nanotubes derived from a natural leucoxene mineral by the hydrothermal method. *Ceram. Int.*, 2014, 40: 9241-9247.
[10] H. Yoo, M. Kim, Y.T. Kim, et al., Catalyst-doped anodic $TiO_2$ nanotubes: Binder-free electrodes for (photo) electrochemical reactions. *Catalysts*, 2018, 8: 555
[11] K.C. Sun, M.B. Qadir, and S.H. Jeong, Hydrothermal synthesis of $TiO_2$ nanotubes and their application as an over-layer for dye-sensitized solar cells. *RSC Adv.*, 2010, 4: 23223-23230.
[12] A. Rydosz, The use of copper oxide thin films in gas-sensing applications. *Coatings*, 2018, 8: 425.
[13] J.A. Losilla, C.Ratanatawanate, and K.J. Balkus Jr, Synthesis of $TiO_2$ nanotube films via pulsed laser deposition followed by a hydrothermal treatment. *Journal of Experimental Nanoscience*, 2014, 9: 126-137.
[14] B. Li, J. Chen, and J.H. Wang, Significantly accelerated osteoblast cell growth on aligned $TiO_2$ nanotubes. *J. Biomed. Mater. Res. A*, 2006, 79: 989-998.
[15] S. Sreekantan, K.A. Saharudin, and L.C. Wei, Formation of $TiO_2$ nanotubes via anodization and potential applications for photocatalysts, biomedical materials, and photoelectrochemical cell. *IOP Conf. Ser. Mater. Sci. Eng.*, 2011, 21.
[16] A.K. Ayal, Z. Zainal, H.N. Lim, et al., Photocurrent enhancement of heat treated CdSe-sensitized titania nanotube photoelectrode. *Optical and Quantum Electronics*, 2017, 49: 164.
[17] Y. Wang, T. Wu, Y. Zhou, et al., $TiO_2$-based nanoheterostructures for promoting gas sensitivity performance: designs, developments, and prospects. Sensors, 2017, 17.
[18] W. Göpel, G. Rocker, and R. Feierabend, Intrinsic defects of $TiO_2$ & (110): Interaction with chemisorbed $O_2$, H&, CO, and $CO_2$. *Phys. Rev. B*, 1983, 28: 3427-3438.
[19] R. Boddula, M.I. Ahamed, and A.M. Asiri, *Inorganic nanomaterials for supercapacitor design*. CRC Press, 2019.
[20] C. Naccache, P. Meriaudeau, M. Che, et al., Identification of oxygen species adsorbed on reduced titanium dioxide. *Trans. Faraday Soc.*, 1971, 67: 506-512.
[21] Y. Gönüllü, G.C.M. Rodríguez, B. Saruhan, et al., Improvement of gas sensing performance of $TiO_2$ towards $NO_2$ by nano-tubular structuring. *Sensors Actuators, B Chem.*, 2012, 169: 151-160.
[22] O.K. Varghese, D. Gong, M. Paulose, et al., Hydrogen sensing using titania nanotubes. *Sensors Actuators, B Chem.*, 2003, 93: 338-344.